IVYSPRING INTERNATIONAL PUBLISHER

Theranostics

2017; 7(7): 2134-2149. doi: 10.7150/thno.17665

Research Paper

Suppression Of β-catenin Nuclear Translocation By CGP57380 Decelerates Poor Progression And Potentiates Radiation-Induced Apoptosis in Nasopharyngeal Carcinoma

Weiyuan Wang[1], Qiuyuan Wen[1], Jiadi Luo[1], Shuzhou Chu[1], Lingjiao Chen[1], Lina Xu[1], Hongjing Zang[1], Mohannad Ma Alnemah[1], Jinghe Li[2], Jianhua Zhou[2], Songqing Fan[1]✉

1. Department of Pathology, Second Xiangya Hospital, Central South University, Changsha, Hunan, 410011, China;
2. Department of Pathology, Xiangya Hospital, Central South University, Changsha, Hunan, 410008, China.

✉ Corresponding author: Department of Pathology, Second Xiangya Hospital, Central South University, Changsha, Hunan, 410011, China. Phone and Fax: 86.731.85292029 E-mail: songqingfan2000@yahoo.com

Received: 2016.09.21; Accepted: 2017.04.08; Published: 2017.05.30

Abstract

Nuclear localization of β-catenin is essential for the progression of various human cancers via transcriptional upregulation of downstream genes. The MAP kinase interacting serine/threonine kinase (MNK)-eukaryotic translation initiation factor 4E (eIF4E) axis has been reported to activate Wnt/β-catenin signaling, and CGP57380, an inhibitor of MNK kinases, inhibits the proliferation of multiple cancers. In this study, we showed that β-catenin signaling (including β-catenin, cyclin D1, c-Myc, and MMP-7) and p-eIF4E expression were elevated in nasopharyngeal carcinoma (NPC) compared with non-cancerous nasopharyngeal epithelial tissues, and was associated with clinical characteristics of NPC patients. Lymph node metastasis, gender, aberrant β-catenin expression, and elevated levels of MMP-7 and cyclin D1 were independent prognostic factors. Significantly, expression of p-eIF4E was positively correlated with β-catenin, and targeting the MNK–eIF4E axis with CGP57380 downregulated β-catenin in the nucleus, which in turn decreased proliferation, cell cycle progression, migration, invasion, and metastasis of NPC in vitro and in vivo. CGP57380 also potentiated radiation-induced apoptosis in NPC. Moreover, CGP57380 upregulated β-catenin in the cytoplasm thus blocking epithelial-mesenchymal transition (EMT), a key mechanism in cancer cell invasiveness and metastasis. Mechanistically, inhibition of β-catenin nuclear translocation by CGP57380 was dependent on AKT activation. Notably, identification of the MNK/eIF4E/β-catenin axis might provide a potential target for overcoming the poor prognosis mediated by β-catenin in NPC.

Key words: nasopharyngeal carcinoma, β-catenin nuclear translocation, CGP57380, poor prognosis, radiation-induced apoptosis.

Introduction

Nasopharyngeal carcinoma (NPC) is a malignant tumor that exhibits significant racial and geographical differences, with a particularly high incidence in Southern China and Southeast Asia. Development and progression of NPC depends on the accumulation of multiple pathogenetic factors, such as Epstein-Barr virus infection, genetic susceptibility, and environmental factors. Although early diagnosis and local control can be achieved, the prognosis for NPC patients with distant metastasis remains poor [1].

The canonical Wnt/β-catenin pathway participates in the pathogenesis of a broad range of

human cancers. β-Catenin, a core component of Wnt/β-catenin signaling, exerts a dual role in cells. Normally, β-catenin functions in formation of the membranous E-cadherin/β-catenin complex that maintains the intercellular tight junction. Minor free β-catenin molecules remaining in the cytoplasm are controlled by multiprotein complexes encompassing kinases, containing glycogen synthase kinase-3β (GSK-3β), casein kinase 1 (CK1), the scaffolding proteins adenomatous polyposis coli (APC) and Axin. In the absence of Wnt ligands, Axin regulates CK1 to initially phosphorylate β-catenin at the Ser45 site [2], followed by phosphorylation of Ser33/37/Thr41 residues mediated by GSK-3β. Phosphorylated β-catenin is targeted for ubiquitination-dependent proteolysis [3-5]. Upon binding of Wnt ligands to the cell surface receptors Frizzled (Fz), phosphorylation of Disheveled proteins with synergistic activity of low-density lipoprotein receptor-related protein (LRP) 5/6 [6] results in stabilization of β-catenin through suppression of GSK-3β activity. The prior study suggested some other mechanisms participated in the regulation of β-catenin stabilization. Wnt could abolish β-transducin repeats-containing proteins (β-TrCP) recruitment to phosphorylated β-catenin preventing β-catenin from ubiquitination and degradation itself [7, 8]. Phosphorylated AKT can also inhibit GSK-3β activity, resulting in the stabilization of β-catenin [9, 10]. In exceptional cases, β-catenin is regulated by AKT-protein phosphatase 2A (PP2A) via phosphorylation of β-catenin at Ser552 and Ser675; this promotes its translocation into the nucleus resulting in activation of T-cell factor (TCF)/lymphoid enhancer factor transcription factors and transcriptional upregulation of downstream genes such as *Ccnd1*, *c-Myc, MMP7* and *AXIN2* [11-14].

The translation initiation factor 4E (eIF4E) is a rate-limiting factor in cap-dependent mRNA translation. eIF4E is specifically phosphorylated at serine 209 by the MAPK interacting kinases (MNK). Targeting the MNK–eIF4E axis by inhibition of MNK kinases is an attractive therapeutic approach given that MNK and eIF4E phosphorylation is dispensable for normal development, but activation of eIF4E and MNK is associated with poor prognosis in numerous human cancers [15]. A small-molecule compound CGP57380 was found to be a potent MNK1 and MNK2 inhibitor in vitro [16, 17]. Our previous study showed that CGP57380 enhanced the efficacy of RAD001 in non-small cell lung cancer through abrogation of mTOR inhibition-induced phosphorylation of eIF4E and activation of the mitochondrial apoptotic pathway [18].

Recent work has highlighted the correlation between the MNK-eIF4E axis and β-catenin signaling. Lim and colleagues reported that the MNK–eIF4E axis activated Wnt/β-catenin signaling by increasing β-catenin mRNA translation and facilitating nuclear translocation of β-catenin protein [19]. Another investigation showed that the antibiotic drug rifabutin targeted human lung cancer cells via inhibition of the eIF4E–β-catenin axis [20]. Although the essential roles of the activated MNK-eIF4E axis and ectopic activation of β-catenin signaling in NPC development have already been identified [21, 22], it is unclear whether there is a direct association between the MNK–eIF4E axis and activated β-catenin in NPC. In the present work, we investigate whether β-catenin signaling is activated in NPC and its relationship to p-eIF4E levels. We also explore whether targeting the MNK-eIF4E axis by CGP57380 can suppress β-catenin nuclear translocation, this decreasing the proliferation, migration, and invasion of NPC in an AKT-dependent manner in vitro and in vivo, and potentiating radiation-induced apoptosis. The identification of a specific MNK–eIF4E–β-catenin axis in NPC may provide a therapeutic window for improving the poor prognosis of this disease.

Material and Methods

Antibodies and reagents are described in detail in the Supplemental Material and Methods.

Cell Lines and Cell Culture

Cell lines used in this study (NP69, CNE1, HNE1, HNE2, 5-8F, and 6-10B) were gifted by the Cancer Research Institute, Central South University. All cell lines were recently authenticated using short tandem repeat (STR) profiling by Microread Gene Technology (Beijing, China). The immortalized NP69 nasopharyngeal epithelial cell line was cultured as described previously [23]. The human NPC cell lines CNE1, HNE1, HNE2, 5-8F, and 6-10B were cultured in RPMI-1640 medium (Hyclone, Logan, UT, USA) supplemented with 10% fetal bovine serum (Hyclone). All cell lines could be revived every 3-4 months from the frozen vial.

Xenograft Mouse Tumor Models

Three previously reported models were used in this study with minor modifications [24, 25]. In the subcutaneous tumor model, CNE1 cells were injected subcutaneously (5×10^6 cells/injection) in 200 μL serum-free medium into male BALB/c nude mice. Tumor growth was monitored by measurement of tumor diameter, and the tumor volume was calculated with the formula $V = (\text{length} \times \text{width}^2)/2$. As soon as the tumor volume reached 50–100 mm^3, the mice were randomly allocated into two groups

(n=6/group) for treatment with vehicle control or CGP57380 (25 mg/kg, three times per week, i.p injection). At the end of treatment, all tumors were excised, weighed, and analyzed by H&E staining and immunohistochemistry (IHC).

In the intravenous injection model, a monoplast suspension containing 5×10^5 CNE1 cells was injected into the tail vein of anesthetized male BALB/c nude mice. Treatment with vehicle control or CGP57380 (25 mg/kg, three times per week, i.p injection) was started immediately after injection (n=3/group). Tumors that developed in the lungs were harvested and confirmed by histology after 3 weeks of treatment.

In the intraperitoneal tumor model, luciferase-expressing CNE1 cells (1×10^7 cells) were injected intraperitoneally into anesthetized male BALB/c nude mice. CGP57380 treatment was initiated when the luminescence signal reached 3×10^6 photons/s. Mice were treated with vehicle control or CGP57380 (25 mg/kg) intraperitoneally three times per week for up to 5 weeks (n=3/group). Development of tumor burden was monitored weekly by bioluminescence imaging (BLI) of anesthetized mice that were intraperitoneally injected with 75 mg/kg D-luciferin (Perkin Elmer). Bioluminescence images were acquired with a Bruker MI SE imaging system. Data were normalized to the weakest signal.

All mice used were of the same age (4 weeks) and similar body weight (20 g). All animal procedures were approved by the Institutional Animal Care and Use Committee of Central South University.

Tissue Specimens

Tissue specimens representing 163 NPC cases were collected at the Second Xiangya Hospital of Central South University (Changsha, Hunan, China) with informed consent from all patients. No patient had previously been treated with radiotherapy and chemotherapy at the time of original biopsy. Complete clinical records and follow-up data were available for all patients and are detailed in Table 1. All specimens had been confirmed by pathological diagnosis according to the World Health Organization histologic classification of NPC. The study was carried out with approval from the Ethics Review Committee of the Second Xiangya Hospital of Central South University. All methods were performed in accordance with the approved guidelines.

Immunohistochemical Staining and Scoring

Immunohistochemical staining for p-eIF4E, β-catenin, cyclinD1, c-Myc, and MMP-7 was performed as previously described [26]. According to a previous investigation, evaluation was based on the intensity and extent of staining [22]. Staining intensity for the above markers except β-catenin was scored as 0 (negative), 1 (weak), 2 (moderate), and 3 (strong), and staining extent was scored as 0 (0%), 1 (≤10%), 2 (11–50%), and 3 (>50%). Marker expression was calculated by multiplying the tumor staining area by the intensity score (0, 1, 2, 3, 4, 6, and 9). Based on research by Li et al. [27], staining scores ≤4 and ≥6 were regarded as low expression and high expression respectively for p-eIF4E, cyclinD1, or MMP-7. Because the expression of c-Myc expression is lower than that of other markers, a staining index score of ≤1 was used to define tumors with low expression while ≥2 indicated high expression. For β-catenin, normal expression was defined as more than 70% of carcinoma cells with positive staining for membranous β-catenin and abnormal expression as more than 10% carcinoma cells showing positive signals in cytoplasm or nuclei [28, 29]. Agreement between the two evaluators was 95%, and all scoring discrepancies were resolved by discussion.

Western Blotting

Protein lysates preparation and western blot analysis were performed as previously described [30].

Growth Inhibition Assay

Cells were plated at 2×10^3 to 4×10^3 cells/well in triplicate 96-well cell culture plates and treated with vehicle or CGP57380 the next day. Live cells were quantified using the sulforhodamine B (SRB) assay, and the percentage of cell proliferation was calculated after 72-h treatment and normalized to the vehicle-treated group. The percentage growth inhibition (GI) was calculated using the equation: %GI = (1-Nt/Nc) ×100, where Nt and Nc represent the absorbance in treated and control cultures respectively. IC50, the drug concentration causing GI of 50%, was determined by interpolation from dose–response curves [31].

β-Catenin-LEF/TCF Regulated Reporter Gene Assay

CNE1 cells were plated at 1.25×10^4 cells/well in triplicate 24-well cell culture plates. The following day, cells were individually co-transfected with TOPFlash or FOPFlash reporter plasmids (17-285, Merck-Millipore) (0.5 μg/well) and equal amounts of pSV-β-galactosidase control vector (E1081, Promega) using Lipofectamine 2000 reagent (11668-019, Invitrogen) according to the manufacturer's instructions. The next day, the cells were trypsinized, washed with serum-free medium, counted, and seeded at 2×10^3 cells per well in 96-well plates. After

cell attachment, DMSO vehicle or CGP57380 was added to the medium to the required concentration. At 24 h after treatment, cells were harvested and analyzed for luciferase activity using the Steady-Glo Luciferase assay system (E2520, Promega) or the β-gal Enzyme Assay System (RG0036, Beyotime). β-catenin activity was calculated by the SuperTOP/FOPflash ratio after normalization to β-gal [32].

Immunofluorescence Staining

Immunofluorescence staining assays were performed as previously described [19]. CNE1 cells (1×10^4) were planted on glass slides in 24-well cell culture plates, fixed with 4% (wt/vol) paraformaldehyde in PBS for 20 min at room temperature, and stained with mouse monoclonal antibodies against β-catenin (8480; Cell Signaling Technology). Slides were then stained with goat anti-rabbit IgG-R (sc-2091; Santa Cruz Biotechnology). Images were obtained with a fluorescence microscope at 400× magnification.

Cytoplasmic and Nuclear Protein Fractionation

The cell fractionation assay was performed as previously described [19].

Cell Cycle Analysis

CNE1 and HNE1 cells were treated with vehicle or the IC50 dose of CGP57380 for 24 h. The PI/RNASE cell cycle assay was performed according to the manufacturer's protocol (550825; BD Pharmingen). Stained cells were analyzed by flow cytometry (FACSCalibur, BD Bioscience, Heidelberg, Germany) using Cell Quest Pro software (BD Bioscience, Heidelberg, Germany).

Wound Healing Assay

A uniform layer of NPC cells was wounded with a 20-μl sterile micropipette tips and washed with serum-free medium to remove detached cells. The remaining cells were treated with or without IC50 values of CGP57380. Photographs of the same area of the wound were taken at 0 h, 24 h, and 48 h to measure the width of the wound.

Matrigel Invasion Assay

Matrigel invasion was measured using a commercially available kit (Transwell; BD Biosciences, San Jose, CA, USA) according to the kit instructions [33]. Briefly, CNE1 and HNE1 cells were suspended in serum-free medium at a density of 1×10^5 cells/mL. One hundred microliters of suspended cells and 100 μL of medium with or without drugs were added to each of the upper chambers (the concentrations of CGP57380 were 20 μM and 50 μM, which were the half of IC50 value). The chambers containing cells were immersed in lower chambers filled with medium containing 10% FBS and incubated for 24 h at 37°C. Non-invading cells that were retained in the upper chamber were removed by cotton swab whereas the invading cells were fixed with 4% (wt/vol) paraformaldehyde in PBS for 20 min at room temperature and stained with 0.1% crystal violet. The number of migrated cells was quantitated using image-Pro plus software over a random composite of five microscopic images (N1, N2, N3, N4, N5), and the values were averaged as (N1+ N2 + N3 + N4+N5) /5.

Migration Assay

The procedures for the migration assay were similar to those described for the Matrigel invasion assay except that no Matrigel was used and the incubation time was 12 h.

Detection of Cell Apoptosis

Detection and analysis of apoptosis by flow cytometry was performed as previously described [18].

Colony Formation and Radiosensitivity Assays

Colony formation and radiosensitivity assays were described previously [23]. Briefly, CNE1 and HNE1 cells were seeded into 6-well plates in triplicates at a density of 1,000cells/well. After 14 days, cells were washed three times with phosphate-buffered saline, fixed in 4% (wt/vol) paraformaldehyde for 10 min, and then stained with 0.1% crystal violet for 20 min at room temperature. Colonies containing more than 50 cells were counted and the surviving fractions were calculated. For the radiosensitivity assay, CNE1 cells were counted and seeded in 6-well plates at densities of 5×10^2, 1×10^3, 5×10^3, or 1×10^4 per well. Cells were pretreated with CGP57380 (25 μM) for 24 h, and then the medium was replaced with complete medium and the cells were treated with radiation (0, 2, 4, or 6 Gy). The colony formation assay was conducted as above and colonies containing more than 50 cells were counted and the surviving fractions calculated. The linear quadratic model was applied for mathematic analysis of radiosensitivity of cells using GraphPad Prism (GraphPad Software, La Jolla, CA, USA).

Quantitative RT-PCR (qRT-PCR) Analysis

Total RNA was extracted using TRIzol reagent (Invitrogen) and 2 μg of total RNA was used for synthesis of first-strand cDNA with a reverse transcriptase kit (Invitrogen). The mRNA level was measured by qPCR with Power SYBR Green qPCR SuperMix-UDG (Invitrogen) on an ABI Prism 7500 HT

sequence detection system (Applied Biosystems, Foster City, CA, USA). Relative expression was determined with a glyceraldehyde-3-phosphate dehydrogenase (GAPDH) control through the $2^{-\Delta\Delta Ct}$ method. The primers used for qRT-PCR are listed in Table S2.

Statistical Analysis

Statistical analyses were performed by log-rank test, Chi-square test, Spearman correlation test, multivariate Cox regression analysis, Pearson correlation, Wilcoxon rank sum test, or student's t-test as appropriate using SPSS for Windows (18.0; SPSS, Inc.) and GraphPad Prism (Prism 5.0; GraphPad Software Inc.) packages. A p value < 0.05 was considered significant. Error bars indicate the standard deviation in all the Figures. *p < 0.05, **p < 0.01, ***p < 0.001 by two-tailed t-test.

Results

β-catenin signaling activates leading to poor prognosis and correlating with eIF4E phosphorylation in NPC

Previous investigation has shown that the levels of β-catenin can be regulated by cap-dependent translation [34]. We performed IHC staining to identify the correlation between p-eIF4E and β-catenin signaling and the subcellular distribution of related proteins (Figure 1A). The results are summarized in Tables 1–3. Specific nuclear and cytoplasmic positive expression of p-eIF4E was observed. The subcellular distribution of β-catenin was found to be heterogeneous throughout each tumor tissue. Positive expression of cyclin D1 and c-Myc was localized in the nucleus, whereas MMP-7 was mainly located in the cytoplasm. Overexpression of p-eIF4E, cyclin D1, c-Myc, and MMP-7 protein was identified in NPC tissues compared with non-cancerous nasopharyngeal epithelial tissues. The rates of positive staining for these four proteins were 68.7%, 42.3%, 41.1%, 42.3% in NPC and 44.1%, 8.8%, 5.9%, and 17.6% in normal tissue, respectively (Figure 1B). Strong membranous β-catenin localization was observed in 100% of noncancerous cases, whereas decreased membranous β-catenin staining, with or without increased cytoplasmic or nuclear β-catenin expression, was observed in NPC cases. Moreover, 72.4% of NPC cases presented abnormal β-catenin expression, compared with only 26.5% of non-cancerous samples. Aberrant β-catenin expression and overexpression of MMP-7 and cyclin D1 were associated with higher clinical stages (p<0.001, 0.003, and 0.003, respectively), lymph node metastasis (LNM) (p < 0.001, 0.005, and 0.012, respectively) and poor survival status (p<0.001, <0.001, and <0.001, respectively) of NPC. Elevated c-Myc expression correlated significantly with severe survival status (p=0.039). Although no significant association was observed between p-eIF4E and clinicopathologic features (p>0.05), common expression of p-eIF4E, β-catenin, MMP-7, cyclin D1, and c-Myc proteins was related to survival status (p=0.037). Interestingly, further analysis of pair-wise associations in NPC indicated positive correlations between overexpression of p-eIF4E and ectopic β-catenin (r=0.205, p<0.01); aberrant β-catenin and elevated MMP-7 (r=0.335, p<0.01), cyclin D1 (r=0.418, p<0.01) or c-Myc (r=0.293, p<0.01); and increased MMP-7 and higher cyclin D1 (r=0.221, p<0.01). Patients with abnormal expression of β-catenin, overexpression of cyclin D1, positive c-Myc, elevated MMP-7, or common ectopic expression of p-eIF4E, β-catenin, MMP-7, cyclin D1, and c-Myc proteins had a shorter survival time (p<0.001, p<0.001, p=0.040, p<0.001, and p< 0.001, respectively) by Kaplan–Meier survival curves and the log-rank test, as did patients with lymph node metastasis (p<0.001) and higher clinical stages (III-IV) (p<0.001) (Figure 1C-J). Multivariate analysis indicated that LNM, gender, aberrant expression of β-catenin, and elevated expression of MMP-7 and cyclin D1 were independent prognostic factors (p=0.003, p=0.027, p=0.002, p=0.003, and p< 0.001, respectively) regardless of age, clinical stage, histological type, p-eIF4E, and c-Myc expression.

We also measured the expression levels of p-eIF4E^{S209}, eIF4E, and β-catenin in a panel of NPC cell lines (5-8F, HNE1, HNE2, CNE1, HK1, and 6-10B) and an immortalized normal nasopharyngeal epithelial cell line (NP69). The results indicated that p-eIF4E and β-catenin expression was higher in NPC cell lines than in the immortalized normal nasopharyngeal epithelial cell line (Figure 1K), and β-catenin expression levels were positively associated with p-eIF4E expression (r=0.921, p=0.003, Figure 1L).

The above data suggest that β-catenin signaling activates leading to poor prognosis. Moreover, p-eIF4E, a crucial element of cap-dependent translation, is involved in the activation of β-catenin. Therefore, we inferred that the eIF4E–β-catenin pathway accelerates the malignant behavior of human NPC.

Table 1. Association between expression of p-eIF4E, β-catenin, MMP-7, cyclin D1 and c-Myc proteins and NPC clinical pathological features (N= 163)

Characteristics(n)	p-eIF4E			β-catenin			MMP-7			cyclinD1			c-Myc			p-eIF4E/β-catenin/MMP-7/cyclinD1/c-Myc*		
	Low (%)	High (%)	*P*	Normal (%)	Abnormal (%)	*P*	Low (%)	High (%)	*P*	Low (%)	High (%)	*P*	N (%)	P (%)	*P*	N- (%)	P+ (%)	*P*
Age(yr)																		
≤40(n=58)	14(24.1)	44(75.9)	0.143	19(32.8)	39(67.2)	0.274	28(48.3)	30(51.7)	0.071	35(60.3)	23(39.7)	0.607	33(56.9)	25(43.1)	0.700	52(89.7)	6(10.3)	0.301[a]
>40(n=105)	37(35.2)	68(64.8)		26(24.8)	79(75.2)		66(62.9)	39(37.1)		59(56.2)	46(43.8)		63(60.0)	42(40.0)		100(95.2)	5(4.8)	
Gender																		
Female(n=36)	15(41.7)	21(58.3)	0.128	14(38.9)	22(61.1)	0.086	25(69.4)	11(30.6)	0.105	22(61.1)	14(38.9)	0.636	20(55.6)	16(44.4)	0.644	33(91.7)	3(8.3)	0.958[a]
Male(n=127)	36(28.3)	91(71.7)		31(24.4)	96(75.6)		69(54.3)	58(45.7)		72(56.7)	55(43.3)		76(59.8)	51(40.2)		119(93.7)	8(6.3)	
Histological type																		
DNC(n=14)	6(42.9)	8(57.1)	0.500[a]	4(28.6)	10(71.4)	1.000[a]	8(57.1)	6(42.9)	0.967	5(35.7)	9(64.3)	0.082	10(71.4)	4(28.6)	0.319	14(100.0)	0(0.0)	0.601[b]
UDNC(n=149)	45(30.2)	104(69.8)		41(27.5)	108(72.5)		86(57.7)	63(42.3)		89(59.7)	60(40.3)		86(57.7)	63(42.3)		138(92.6)	11(7.4)	
Clinical Stages																		
StagesI-II(n=67)	22(32.8)	45(67.2)	0.722	34(50.7)	33(49.3)	< 0.001*	48(71.6)	19(28.4)	0.003*	48(71.6)	19(28.4)	0.003*	39(58.2)	28(41.8)	0.882	64(95.5)	3(4.5)	0.517[a]
Stages III-IV(n=96)	29(30.2)	67(69.8)		11(11.5)	85(88.5)		46(47.9)	50(52.1)		46(47.9)	50(52.1)		57(59.4)	39(40.6)		88(91.7)	8(8.3)	
LN Status																		
LNM(n=105)	33(31.4)	72(68.6)	0.959	12(11.4)	93(88.6)	< 0.001*	52(49.5)	53(50.5)	0.005*	53(50.5)	52(49.5)	0.012*	60(57.1)	45(42.9)	0.541	99(94.3)	6(5.7)	0.702[a]
No LNM(n=58)	18(31)	40(69)		33(56.9)	25(43.1)		42(72.4)	16(27.6)		41(70.7)	17(29.3)		36(62.1)	22(37.9)		53(91.4)	5(8.6)	
Survival Status																		
Alive(n=79)	29(36.7)	50(63.3)	0.148	42(53.2)	37(46.8)	< 0.001*	59(74.7)	20(25.3)	< 0.001*	62(78.5)	17(21.5)	< 0.001*	53(67.1)	26(32.9)	0.039*	77(97.5)	2(2.5)	0.037*
Dead(n=84)	22(26.2)	62(73.8)		3(3.6)	81(96.4)		35(41.7)	49(58.3)		32(38.1)	52(61.9)		43(51.2)	41(48.8)		75(89.3)	9(10.7)	

Abbreviations:

DNC: Differentiated non-keratinized nasopharyngeal carcinoma, UDNC: Undifferentiated non-keratinized nasopharyngeal carcinoma, LN: lymph node. n, Number of cases

*: statistically significant ($p < 0.05$), statistical analysis was performed using the Chi-squared test.

+: Common positive staining of five proteins, -: any negative expression of five proteins.

a: Continuity correction of Chi-squared-value

b: DNC versus UDNC, Fisher's exact test

Table 2. The pairwise association between expression of β-catenin, p-eIF4E, MMP-7, cyclinD1 and c-Myc proteins in the 163 cases of NPC

	p-eIF4E	β-catenin	MMP-7	cyclinD1	c-Myc
p-eIF4E	1	0.205**	0.096	0.069	0.080
β-catenin	-	1	0.335**	0.418**	0.293**
MMP-7	-	-	1	0.221**	0.016
cyclinD1	-	-	-	1	0.016

NOTE: Values are Spearman correlation coefficient. ** Correlation is significant at the P<0.01 level (2 tailed).

Table 3 Summary of multivariate analysis of Cox proportional hazard regression for overall survival in 163 cases of NPC

Parameter	SE	Wald	Sig.	Exp(B)	95.0% CI for Exp(B) Lower	Upper
Age	0.261	1.632	0.201	1.396	0.837	2.331
Gender	0.277	4.894	0.027*	0.542	0.315	0.932
Histological types	0.388	2.744	0.098	0.526	0.246	1.125
LNM status	0.340	8.586	0.003*	0.370	0.190	0.719
Clinical stages	0.326	2.259	0.133	1.632	0.862	3.090
p-eIF4E^{S209}	0.262	2.199	0.138	1.475	0.883	2.465
β-catenin	0.623	9.670	0.002*	6.946	2.047	23.566
MMP-7	0.230	8.593	0.003*	1.961	1.250	3.076
cyclinD1	0.233	13.461	0.000*	2.351	1.489	3.711
c-Myc	0.234	2.519	0.113	1.451	0.916	2.297

Abbreviations: LNM, lymph node metastasis; CI, confidence interval.

Note: multivariate analysis of Cox regression, *: p<0.05

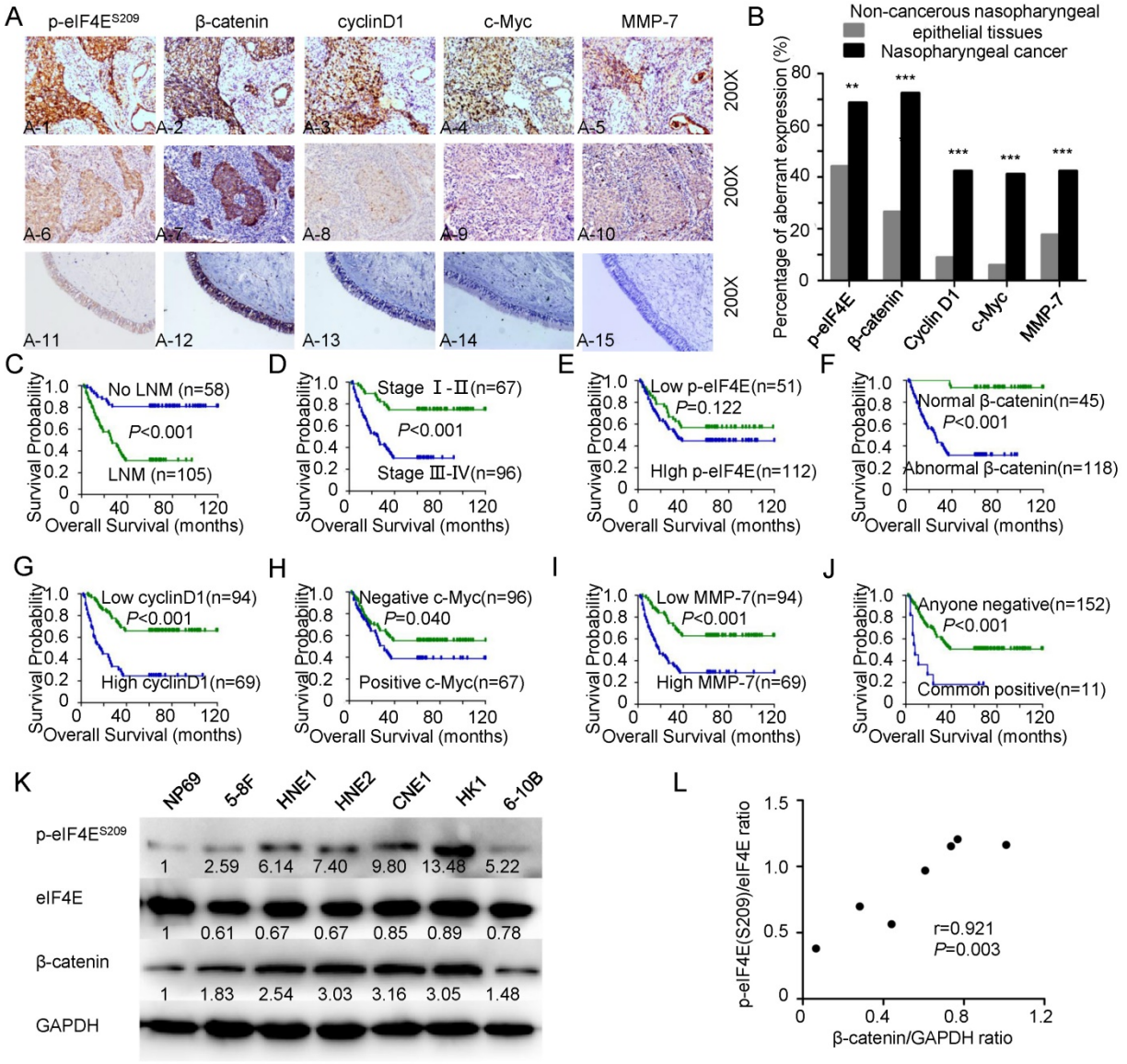

Figure 1. β-catenin signaling activates leading to poor prognosis and correlating with eIF4E phosphorylation in NPC A: Representative immunohistochemical staining of p-eIF4E, β-catenin, cyclin D1, c-Myc, and MMP-7 in NPC cases and non-cancerous nasopharyngeal epithelial tissues (all images, 200×). β-catenin is mainly located in the cytoplasm or in the nucleus, together with overexpressed cyclin D1, c-Myc, and MMP-7 when is p-eIF4E elevated (A1-5). p-eIF4E is weakly expressed in the NPC cases with strong membranous β-catenin localization and weak expression of cyclin D1, c-Myc, and MMP-7 (A6-10). Low staining of p-eIF4E, β-catenin, cyclin D1, c-Myc, and MMP-7 was observed in the control nasopharyngeal epithelia (A11-15). B: Expression of p-eIF4E, β-catenin, cyclin D1, c-Myc, and MMP-7 in NPC compared with non-cancerous nasopharyngeal epithelial tissues. The P values were determined by chi-square analysis. *$p < 0.05$, **$p < 0.01$, ***$p < 0.001$, by two-tailed t test. C-J: Kaplan–Meier analysis was used to plot the overall survival curves of 163 NPC patients with different LNM status, clinical stages, expression of p-eIF4E, β-catenin, cyclin D1, c-Myc, and MMP-7 and combined expression of five proteins above; statistical significance was assessed by log-rank test. K: Western blot analysis of p-eIF4E^{S209}/eIF4E and β-catenin levels in NPC cell lines (5-8F, HNE1, HNE2, CNE1, HK1, and 6-10B) and an immortalized normal nasopharyngeal epithelial cell line (NP69). L: Correlation between p-eIF4E^{S209}/eIF4E ratio and β-catenin/GAPDH ratio.

Targeting the MNK-eIF4E axis by CGP57380 regulates the expression of β-catenin signaling factors

β-catenin signaling is aberrantly activated in NPC. To evaluate targeting the MNK-eIF4E axis by CGP57380 as a promising therapeutic strategy through control of β-catenin distribution, we inactivated eIF4E using CGP57380. Proliferation of NPC cell lines was inhibited by CGP57380 in a concentration-dependent manner over the range of 0 to 100 μM CGP57380, as measured by 3-day cell survival assay (Figure 2A, left). Only treatment with a higher dose of CGP57380 suppressed the proliferation of NP69 cells; the IC50 for CGP57380 in NP69 cells was 273.44 μM, compared with 38.261 μM, 82.042 μM, 103.278 μM, 13.532 μM and 89.416 μM for CNE1, HNE2, HNE1, HK1, or 6-10B cell lines respectively (Figure 2A, right). Heterogeneous sensitivity to CGP57380 positively correlated with p-eIF4E levels of NPC cell lines (Figure 2B). Among the above NPC cell lines that were sensitive to CGP57380, the well-differentiated squamous cancer cell line CNE1 and the poorly differentiated squamous cancer cell

line HNE1 were chosen as candidates for follow-up studies.

Clonogenic assays are regarded the "gold standard" for measuring cellular sensitivity to drug treatment [35]. The IC50 dose of CGP57380 abolished the clonogenicity of CNE1 and HNE1 cell lines (Figure 2C). The colony number decreased compared with vehicle-treated groups due to slow growth of the surviving cells. Using a TCF reporter assay, we discovered that β-catenin transcriptional activity was regulated by CGP57380 concentration (Figure 2D). Interestingly, targeting the MNK–eIF4E axis decreased the expression of p-MNK1 and p-eIF4E and the mRNA and protein expression of factors downstream of β-catenin signaling including c-Myc, cyclin D1, MMP-7, and Axin2, but increased the expression of β-catenin (Figure 2E-F & S1A-B), which was inconsistent with IHC data and previous results. Using a series of tests, we showed that the activity of β-catenin signaling relies on accumulation of translocated β-catenin in the nucleus, one of the hallmarks of the initiation of tumorigenesis in a broad spectrum of human cancers [36-38]. Thus, to study the effect of CGP57380 on β-catenin expression, the distribution of β-catenin must be examined.

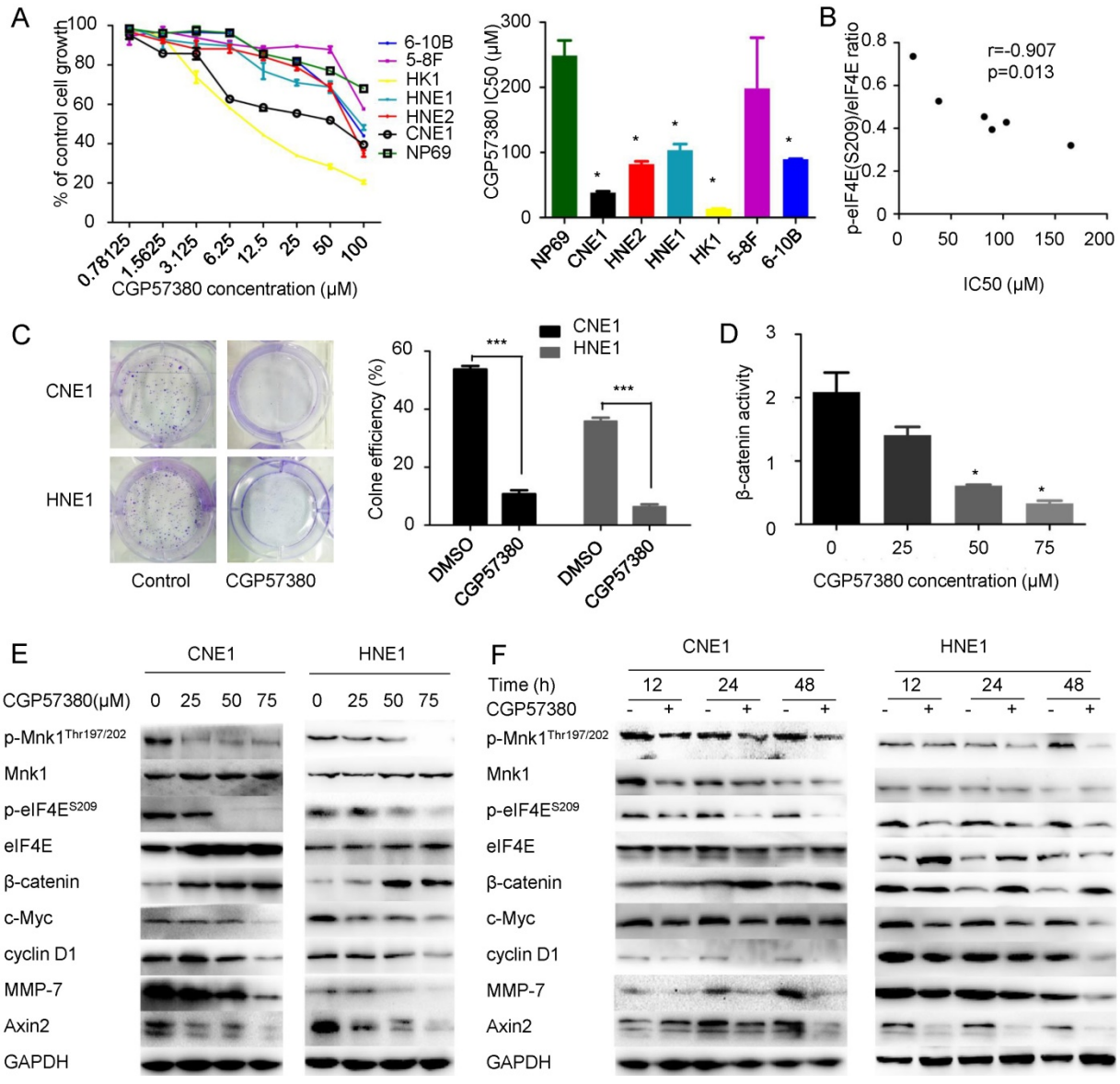

Figure 2. Targeting MNK-eIF4E axis by CGP57380 regulates β-catenin signaling factors A: (*Left*) Cell viability assay in six NPC cell lines and an immortalized normal nasopharyngeal epithelial cell line treated with CGP57380 at various concentrations for 3 days. (*Right*) Densitometric readings for IC50 values of NPC cells compared with the IC50 value of an immortalized normal nasopharyngeal epithelial cell line; mean ± SD; **p*<0.05. B: Correlation between p-eIF4E (S209)/eIF4E ratio and IC50 of CGP57380. C: (*Left*) Clonogenic assay. The cells were exposed to CGP57380 (control, and IC50) for 14 days, and representative plates were photographed. (*Right*) Clone formation efficiency (CFE) was calculated as a ratio of the number of colonies to total cells plated. Colonies containing more than 50 cells were counted; means ± SD from three independent experiments are presented; ****p*<0.001. D: TCF reporter assays were performed on CNE1 cells treated with DMSO or CGP57380 at increasing concentrations for 24 h. E: MNK–eIF4E axis and downstream targets of β-catenin signaling including c-Myc, cyclin D1, MMP-7, and Axin2 were downregulated, whereas β-catenin level was upregulated by treatment with gradient concentration of CGP57380 for 24 h in CNE1 and HNE1 cell lines. F: Inhibition of MNK–eIF4E axis, suppression of downstream targets of β-catenin signaling, and elevated β-catenin levels in CNE1 and HNE1 cell lines by CGP57380 at IC50 in a time-dependent manner.

CGP57380 regulates β-catenin distribution in NPC cells leading to alteration of epithelial-mesenchymal transition morphology, cell cycle arrest and inhibition of migration and invasion

To further investigate the distribution of β-catenin, we measured the β-catenin level in cytosolic and nuclear extracts of CNE1 and HNE1 cell lines following CGP57380 treatment. Western blot data showed that β-catenin nuclear translocation was suppressed by CGP57380 but β-catenin accumulated in the cytoplasm compared with the untreated control cells (Figure 3A). Immunofluorescent staining indicated that the active β-catenin was predominantly localized around the membrane, making tight intercellular junctions much more compact (Figure 3B, left). We also found that β-catenin nuclear translocation was suppressed by CGP57380 in a dose-dependent manner (Figure 3B, right; and Figure 3C). The redistribution of β-catenin led to altered epithelial-mesenchymal transition (EMT) morphology of NPC cells, together with increased levels of E-cadherin and decreased expression of Vimentin, N-cadherin, and slug (Figure 3D & S1C-D).

CGP57380-mediated regulation of β-catenin distribution resulted in changes in related proteins in CNE1 and HNE1 cell lines, which in turn induced alteration of EMT morphology, cell cycle arrest (Figure 3E) and inhibited migration (2D and 3D) and invasion (Figure 3F-G) in NPC cells.

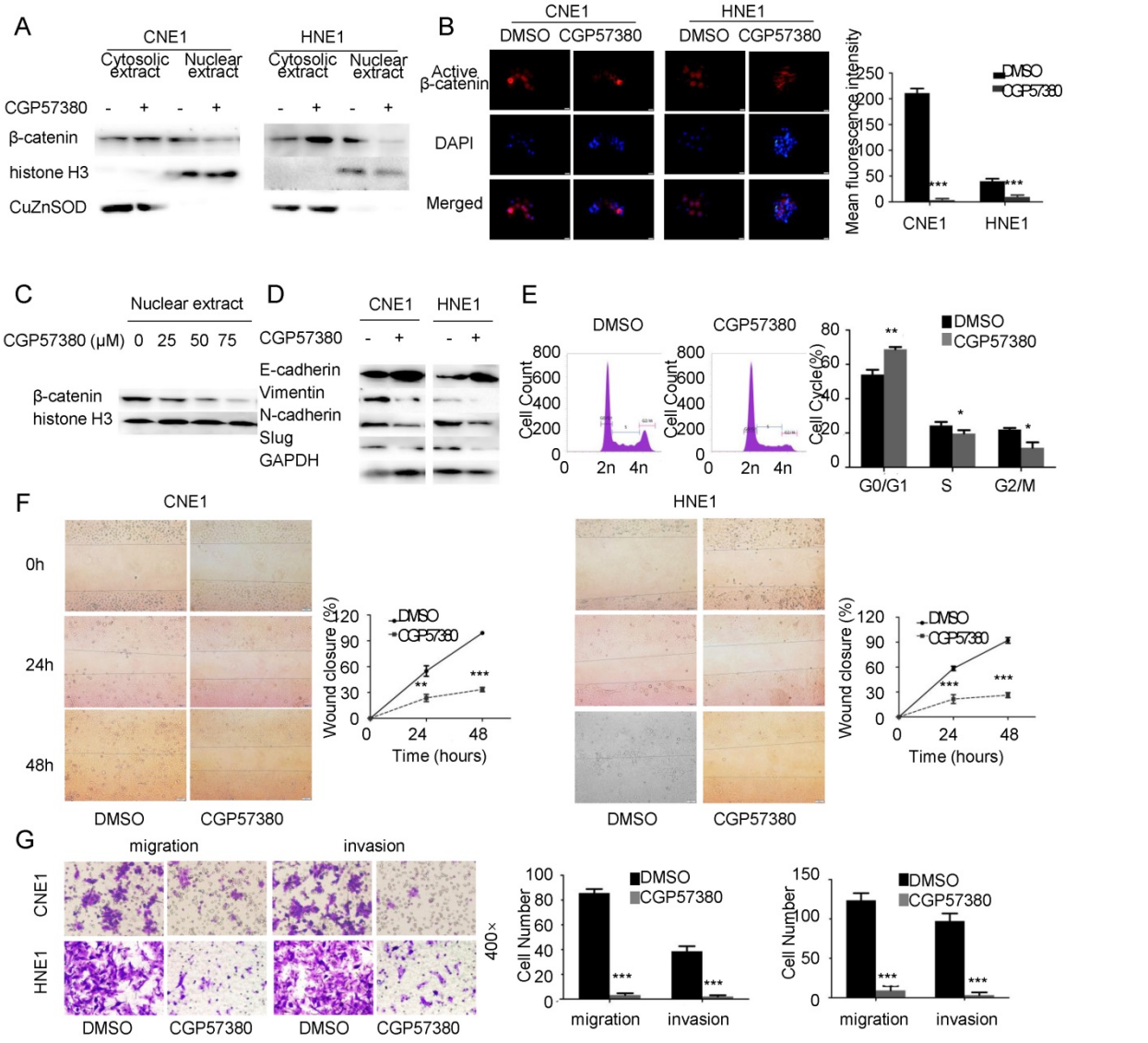

Figure 3. CGP57380 regulates β-catenin distribution in NPC cells leading to alteration of epithelial-mesenchymal transition morphology, cell cycle arrest and inhibition of migration and invasion A: CGP57380 suppressed the nuclear translocation of β-catenin and promoted accumulation of β-catenin in the cytoplasm in CNE1 and HNE1 cell lines. Antibodies to histone H3 and CuZnSOD were used to confirm nuclear/cytosolic protein separation, respectively. B: Active β-catenin in cytoplasm was mainly distributed near the cell membrane as verified by immunofluorescence staining. C: CGP57380 inhibited the nuclear translocation of β-catenin in a concentration-dependent manner. D: CGP57380 increased expression of E-cadherin and decreased expression of Vimentin, N-cadherin, and slug in CNE1 and HNE1 cell lines. E-G: NPC cells showed cell cycle arrest and inhibition of migration (2D & 3D) and invasion.

CGP57380 inhibits growth and metastasis of NPC *in vivo*

Promotion of cellular proliferation, migration, and EMT are important functions of β-catenin signaling in cancers [39-41]. To examine the therapeutic potential of CGP57380 for the development of NPC in vivo, we next examined its capacity to suppress tumor growth and metastatic potential using three established murine xenograft models of NPC. CNE1 cells were employed in xenograft experiments in BALB/c nude mice. In the subcutaneous model, the volume (Figure 4A) and weight (Figure 4C) of tumors were significantly decreased in the CGP57380-treated group compared with the control group without obvious toxicity and body weight change (Figure 4B). The relative tumor growth curves for control and CGP57380-treated animals are shown in Figure 4D. The CGP57380-treated group showed significantly reduced tumor growth compared with the control group (p=0.016). In agreement with our in vitro studies, the expression of Ki-67, p-eIF4E, and downstream targets of β-catenin signaling (including cyclin D1, c-Myc, and MMP-7) in CNE1 xenografts was significantly reduced in the CGP57380-treated group as measured by IHC (Figure 4E and Figure S3). The intraperitoneal model was used to determine whether CGP57380 was effective in suppressing intraperitoneal tumor growth. CNE1 cells were injected intraperitoneally in a new cohort of mice followed by treatment with either vehicle or CGP57380. Tumor involvement was observed in the scrotum and abdominal muscle in both groups, but in spleen, liver, kidney, and diaphragmatic muscle only in the vehicle group. Tumor burden and the capacity for invasion and metastasis of the CNE1 cells were significantly decreased by CGP57380 (Figure 4F-H). Expression of E-cadherin increased and that of Vimentin decreased in CGP57380-treated tumors of abdominal muscle, as detected by IHC in abdominal muscle metastases of NPC tissues (Figure 4I). In the intravascular model CNE1 cells were injected via the tail vein into BALB/c nude mice and metastasis loci were detected in the lungs of the control vehicle-treated group, but not in the CGP57380-treated mice (Figure 4J).

These results demonstrated that targeting the MNK–eIF4E axis by CGP57380 inhibited growth and metastasis of NPC in vivo.

CGP57380 potentiates radiation-induced apoptosis in nasopharyngeal carcinoma

Growing evidence indicates that eIF4E and nuclear β-catenin exert essential roles in radiotherapy resistance. Yu et al. found that eIF4E phosphorylation induced by the caspase 3/PKCδ/p38/MNK1 signaling pathway was required for Sox2 upregulation, which in turn promoted recurrence in pancreatic tumor cells treated with radiotherapy [42]. Nuclear β-catenin overexpression is more evident in radioresistant rectal adenocarcinoma than in radiosensitive rectal adenocarcinoma [43]. To test the effect of targeting the MNK–eIF4E–β-catenin axis by CGP57380 on the sensitivity of NPC cells to radiation therapy, NPC cells were pretreated with vehicle or CGP57380 and then left untreated or irradiated. The results of an SRB assay suggested that concomitant treatment with the MNK inhibitor CGP57380 and radiotherapy significantly decreased the viability of all tested cell lines compared with other treatments, with a synergistic effect (p<0.001, Figure 5A). The radiosensitivity of CNE1 cells with or without CGP57380 pretreatment was evaluated after irradiation at a single dose of 0, 2, 4, or 6 Gy. CGP57380 pretreatment had a greater inhibitory effect on colony formation and resulted in a lower survival rate after irradiation compared with cells treated with irradiation only (Figure 5B). As apoptosis is a major form of cell death induced by irradiation, we performed flow cytometry using Annexin V/PI staining to assess apoptosis in CNE1 and HNE1 cell lines treated with vehicle, CGP57380, radiotherapy, vehicle combined with radiotherapy, or CGP57380 combined with radiotherapy. The results indicated that CGP57380-pretreated NPC cells were more susceptible to undergo early apoptosis induced by irradiation than the other groups (p<0.001, Figure 5C). In parallel, western blot analysis showed that radiotherapy-treated CNE1 and HNE1 cells showed activated eIF4E and elevated cyclin D1 expression compared with untreated controls. Targeting the MNK–eIF4E–β-catenin axis by CGP57380 abrogated the activation of eIF4E and inhibited expression of cyclin D1. Concomitant treatment with MNK inhibitor CGP57380 and radiotherapy resulted in more obvious p-eIF4E and cyclinD1 inhibition, and induced higher expression of cleaved PARP, indicating more damage in the DNA of irradiated cells (Figure 5D). eIF4E was significantly activated when CNE1 and HNE1 cell lines were exposed to combined treatment of DMSO and radiotherapy. Previous studies reported that DMSO could protect cells from radiation damage and facilitate the DNA double-strand break repair system [44]. Therefore, we inferred that eIF4E activation might be the critical radioprotective mechanism of DMSO, but further research to validate this notion is needed.

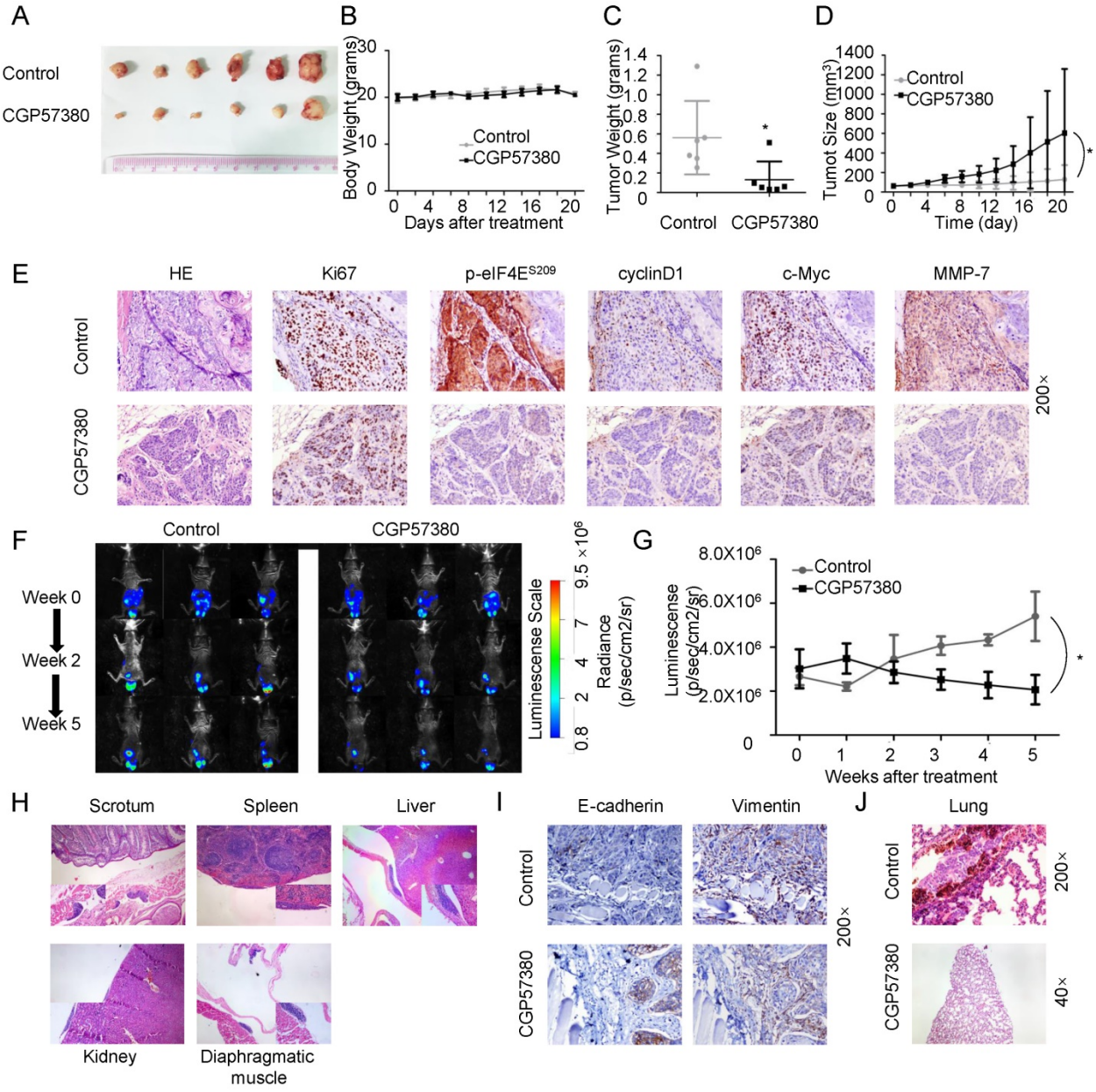

Figure 4. CGP57380 inhibits growth and metastasis of NPC *in vivo* A: Photographs of tumors from mice treated with control vehicle or CGP57380. B: The weight of nude mice was monitored every 2 days. C: Weight of tumors after mice were sacrificed, *$p<0.05$. D: Growth curves of CNE1 tumors in the presence of CGP57380, *$p<0.05$. E: H&E staining (top) and immunohistochemical staining for Ki-67, p-eIF4E, cyclin D1, c-Myc, and MMP-7 in control and CGP57380-treated tumors. See also Figure S3. F-G: Luminescence signals and analysis of intraperitoneal CNE1-Luc tumor xenografts from different treatment groups at the indicated week, *$p<0.05$. Results are shown as the mean ± SD. See also Figure S6. H: Migration of intraperitoneal CNE1-Luc tumor xenografts in the surface of abdominal organs. I. Increased E-cadherin and decreased vimentin expression in CGP57380-treated tumors of abdominal muscle. J: Representative H&E images of lung metastatic lesions of intravenously injected mice.

Regulation of the distribution of β-catenin by CGP57380 is dependent on AKT activation

To better understand the role of targeting the MNK–eIF4E axis by CGP57380 in the suppression of β-catenin nuclear translocation, we noted the main findings of two previous studies showing that eIF4E phosphorylation leads to AKT activation, which in turn promotes β-catenin signaling [19], and that AKT-mediated phosphorylation of β-catenin at serine 552 (S552) is a necessary step in β-catenin nuclear translocation and activation [10]. These results suggest a model in which eIF4E phosphorylation mediates β-catenin nuclear translocation in an AKT-dependent manner. Therefore, we assessed the levels of p-eIF4E^{S209}/eIF4E, p-AKT^{S473}/AKT, and p-β-catenin^{S552}/β-catenin in CNE1 cells after treatment with vehicle, MNK inhibitor CGP57380, AKT inhibitor MK2206, combined treatment with CGP57380 and MK2206, AKT activator IGF-1, combined treatment with CGP57380 and IGF-1, Wnt inhibitor XAV939, or combined treatment with CGP57380 and XAV939. We found that only CGP57380 inhibited p-eIF4E expression. Activation of

AKT and β-catenin in CNE1 could be abrogated by CGP57380 through blocking eIF4E phosphorylation. The inhibitory effect of CGP57380 on p-AKT and p-β-catenin^{S552} could be enhanced by MK2206 but was reversed by IGF-1. Both MK2206 and IGF-1 did not show any significant effect on the expression of p-eIF4E. We therefore thought that p-eIF4E activated AKT, and AKT-dependent enhancement of β-catenin S552 phosphorylation promoted nuclear translocation of β-catenin in NPC cells. XAV939 inhibited β-catenin expression, but had no effect on p-eIF4E^{S209}/eIF4E and p-AKT^{S473}/AKT. Complementary to XAV939, CGP57380 could further prevent β-catenin nuclear translocation by the regulation of AKT activation inhibited by eIF4E. Only inactivation of eIF4E by CGP57380 could promote the accumulation of β-catenin in the cytosol. Moreover, TCF transcriptional activity and the capacity of migration and invasion changed according to the nuclear expression of β-catenin; high β-catenin expression in the nucleus resulted in higher transcriptional activity and stronger capacity of migration and invasion (Figure 6B-C & S4).

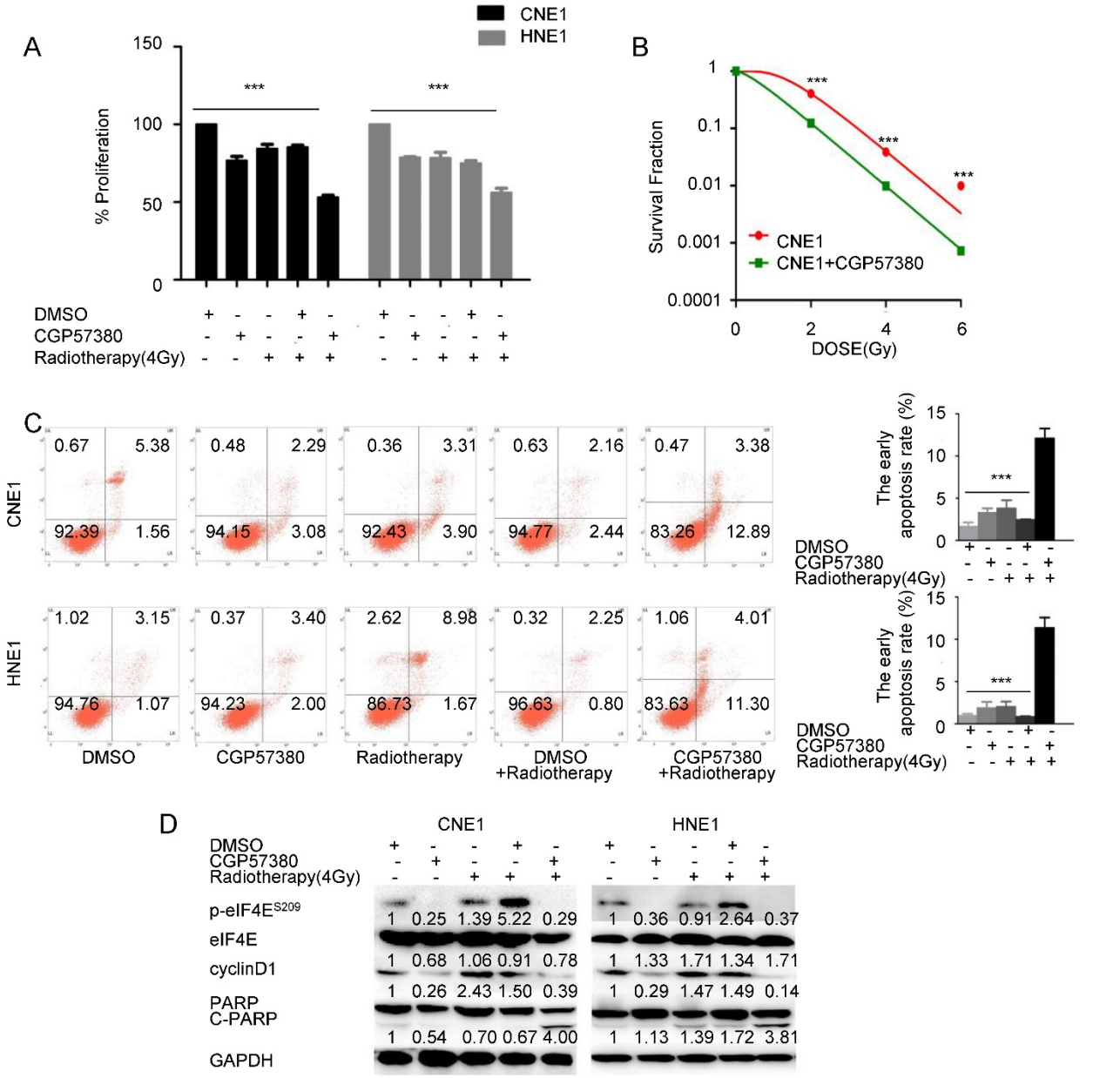

Figure 5. Targeting the MNK–eIF4E–β-catenin axis by CGP57380 enhances the antiproliferative effects of radiation in NPC cell lines by inducing apoptosis A: Effect of CGP57380 on the sensitivity of NPC cells to radiotherapy was evaluated by sulforhodamine B assay (SRB). Concomitant treatment with MNK inhibitor CGP57380 and radiotherapy significantly decreased the viability of all tested cell lines compared with other treatments, with a synergistic effect. B: Colony formation ability of CNE1 cells with or without CGP57380 was measured 14 days after radiation at a single dose of 0, 2, 4, or 6 Gy. See also Figure S5. Surviving fraction was calculated. C: Measurement of early apoptotic CNE1 and HNE1 cells 48 h after radiation with or without CGP57380 pretreatment as assessed by flow cytometry. CGP57380-pretreated NPC cells were more susceptible to early apoptosis induced by irradiation than other groups. D: Western blot analysis of p-eIF4E, cyclin D1, and cleaved PARP after radiation with or without CGP57380 pretreatment in CNE1 and HNE1 cells. * $p<0.05$, ** $p<0.01$ ***$p<0.001$. Each bar represents mean ± SD.

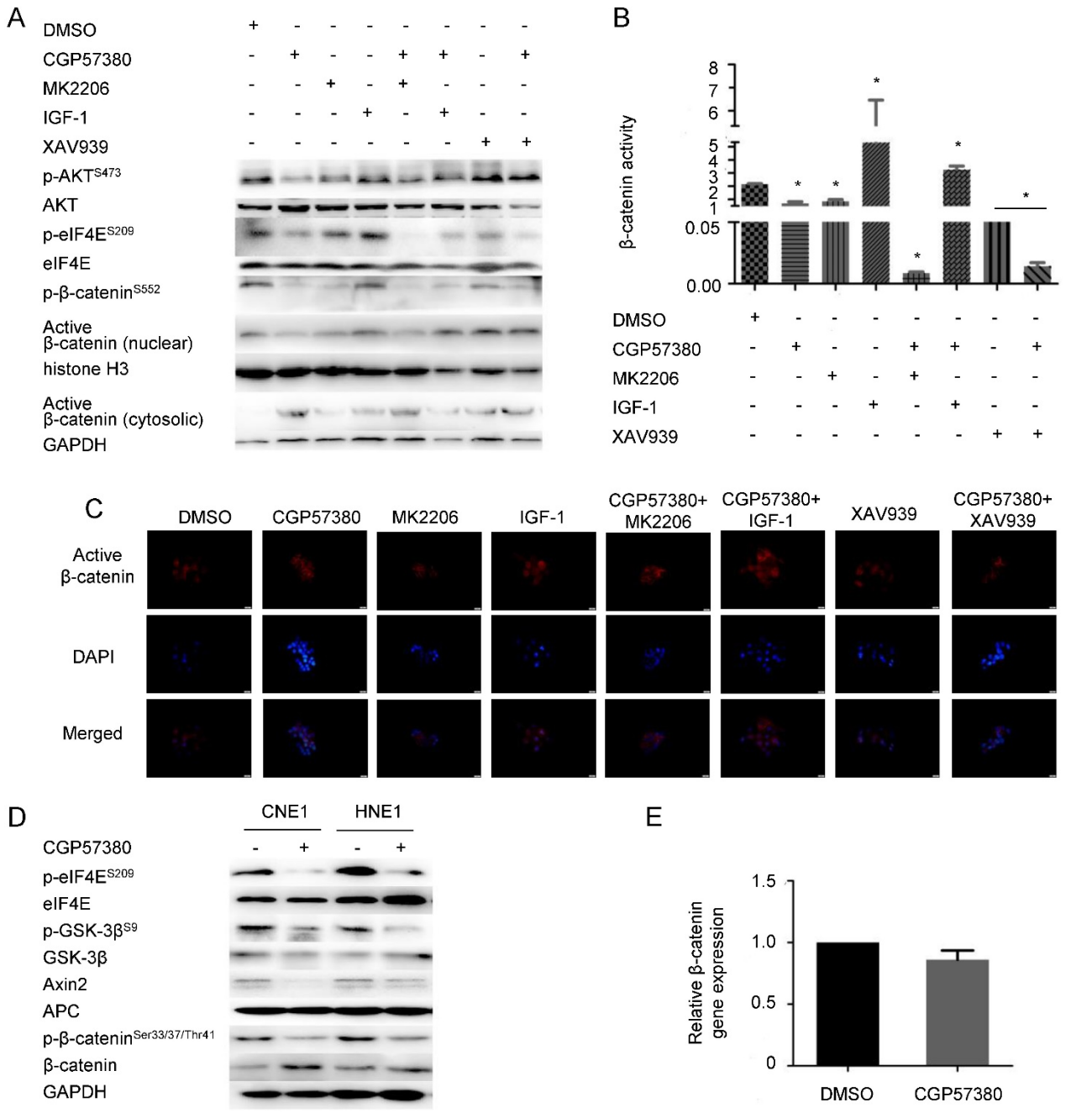

Figure 6. Inhibition of β-catenin nuclear translocation by CGP57380 is dependent on AKT activation A: Western blot analysis of cell lysates from CNE1 cells treated with DMSO, MNK inhibitor CGP57380, AKT inhibitor MK2206, AKT activator IGF-1, combined treatment with CGP57380 and MK2206, combined treatment with CGP57380 and IGF-1, Wnt inhibitor XAV939, or combined treatment with CGP57380 and XAV939 for 24 h. B: TCF reporter assays were performed on CNE1 cells treated as in A. C: The distribution of active β-catenin in CNE1 cells treated as in A. D: Regulation of β-catenin degradation by ubiquitination in NPC cells treated with CGP57380. E: qRT-PCR analysis of *β-catenin* transcription.

Regarding accumulation of β-catenin in the cytoplasm, when AKT/GSK-3β was suppressed by CGP57380, phosphorylation of β-catenin (Ser33/37/Thr41), a downstream target of AKT/GSK-3β, decreased resulting in a reduction in the ubiquitination-mediated degradation of β-catenin in CNE1 and HNE1 cells (Figure 6D). This contradicts other findings. A previous study showed that Wnt/β-catenin/Tcf signaling induced transcription of Axin2, which could be a negative regulator of the signaling pathway [45]. Coincidently, Axin2 expression was inhibited by CGP57380. Besides, we also observed no difference in β-catenin transcription in CGP57380-treated versus control cells (Figure 6E). We propose that downregulation of Axin2 prevented ubiquitination of β-catenin, which subsequently accumulated in the cytoplasm [45].

Discussion

As a result of a combination of lifestyle modification and population screening coupled with better imaging, advances in radiotherapy, and more effective systemic agents, the incidence and mortality of NPC is gradually declining, even in endemic regions (see review in ref. [46]). Nevertheless, effective treatment for nasopharyngeal carcinoma with local residual or distant metastasis remains an unmet need in the developing world. New strategies including molecular-targeted therapies, such as inhibition of epidermal growth factor receptor (EGFR) or vascular endothelial growth factor (VEGF), have yielded impressive disease control in preclinical studies of NPC [47-49].

In the present study, we found that increased eIF4E phosphorylation at S209 and overexpressed β-catenin were consistent features in the 163 NPC tissues and 6 NPC cell lines tested, together with a positive correlation between β-catenin levels and p-eIF4E expression. In addition, lymph node metastasis, gender, aberrant expression of β-catenin, and elevated expression of MMP-7 and cyclin D1 were independent prognostic factors. Notably, Lim et al. demonstrated that eIF4E phosphorylation is necessary for β-catenin activation and nuclear localization [19], and Karni et al. reported that enhancement of phosphorylated eIF4E results in the accumulation of certain proteins, such as the β-catenin transcription factor [34]. We further revealed that the MNK–eIF4E–β-catenin axis in NPC is a critical factor in poor prognosis (higher clinical stages, lymph node metastasis, and poor survival status). As for the relationship between patient survival and the expression of p-eIF4E, we took note of an early finding that normal development and cancer had differential requirements for eIF4E dose [50]. In addition, the regulatory network of eIF4E activation could affect p-eIF4E expression. Thus, we speculated that the regulation of ectopic p-eIF4E might be more complicated, so it was not sufficient to directly affect the survival of NPC patients.

We exposed a range of NPC cell lines and immortalized normal nasopharyngeal epithelial cell line to CGP57380 and observed that targeting the MNK–eIF4E axis by CGP57380 treatment decreased their proliferation and colony-forming ability with little apparent toxicity to the immortalized normal nasopharyngeal epithelial cell line, which was consistent with previous investigations in blast crisis chronic myeloid leukemia and NSCLC [18, 51]. Paradoxically, when expression of p-MNK1 and p-eIF4E was inhibited by CGP57380, the expression of total β-catenin was stimulated but the downstream targets of β-catenin signaling, including cyclin D1, c-Myc, MMP-7, and Axin2, were suppressed in a time- and dose-dependent manner. Moreover, we found that β-catenin accumulated only in the cytoplasm, where it enhanced intercellular adhesion and reduced migration of NPC cells, together with increased expression of E-cadherin and decreased expression of Vimentin, N-cadherin and slug, which terminated EMT, a key mechanism in cancer cell invasiveness and metastasis. Nuclear translocation of β-catenin was suppressed, leading to inhibition of the downstream targets cyclin D1, c-Myc, and MMP-7. MMP-7 is a matrix metalloproteinase (MMP) with wide proteolytic activity for degradation of extracellular matrix proteins and activation of other MMPs. Downregulation of MMP-7 impairs the capability of the cell for invasion and metastasis. Cyclin D1 and c-Myc are significant participants in cell proliferation and differentiation. Inhibition of these molecules by CGP57380 induces cell cycle arrest and blocks cellular proliferation. The activity of β-catenin signaling relies on the translocation and accumulation of β-catenin in the nucleus, one of the hallmarks of tumorigenesis in multiple human cancers [52, 53]. As a transcription factor, β-catenin is involved in carcinogenesis and metastasis through regulating the expression of downstream molecules in the nucleus [54]. We demonstrated that CGP57380 could prevent translocation of β-catenin into the nucleus and enhance recruitment of β-catenin in cytoplasm. In this way, CGP57380 suppresses the progression of NPC by direct inhibition of nuclear β-catenin signaling and by maintaining the adhesion between cells. Thus, targeting the MNK–eIF4E axis may ameliorate the poor progression of NPC mediated by β-catenin activation.

Our work also elucidated the mechanisms by which CGP57380 prevents nuclear translocation of β-catenin. In the NPC cell lines, AKT phosphorylation at S473 and β-catenin phosphorylation at S552 were inhibited by CGP57380 through inhibition of eIF4E phosphorylation at S209. This phenomenon could be reversed by the AKT agonist IGF-1 and enhanced by the AKT inhibitor MK2206. When AKT was phosphorylated by IGF-1, β-catenin was phosphorylated at S552 and translocated into nucleus to initiate the transcription of tumor-associated genes. The above data suggest that inhibition of β-catenin nuclear translocation by CGP57380 is dependent on AKT activation in NPC cell lines. With respect to regulation of the accumulation of β-catenin in the cytoplasm by CGP57380, we focused on expression of Axin2, which is believed to function by promoting phosphorylation at S33/37/Thr41 sites of β-catenin and its consequent degradation. We observed that

CGP57380 suppressed Axin2 expression, preventing β-catenin phosphorylation at S33/37/Thr41 sites without obvious inhibition of relative β-catenin gene expression. This resulted in accumulation of β-catenin in the cytoplasm and cytomembrane and repressed the invasive mesenchymal phenotype in NPC.

Yang *et al.* discovered that CGP57380 abrogated eIF4E phosphorylation-mediated repopulation and prevented recurrence in irradiated pancreatic tumor cells [42]. Overexpression of nuclear β-catenin is associated with radioresistance in human cervical squamous cell cancer and rectal adenocarcinoma [43, 55]. Therefore, we inferred that CGP57380 exerted the dual function of sensitizing NPC cells to radiation. CGP57380 pretreatment of NPC cell lines exhibited more obvious inhibition of proliferation than other treatments, mainly through induction of apoptosis as assessed by flow cytometry and c-PARP expression. Growing cells double their volume during G1 and G2 phase so that the cell volume is conserved in mitosis. Cells in the G2 phase are considered radioresistant because of lingering enzymes and CDK complexes from S phase. The suppression of nuclear β-catenin by CGP57380 resulted in downregulation of cyclin D1 expression, limiting its level in cells in G0/G1 phase and sensitizing the cells to radiation therapy.

In summary, we demonstrated that CGP57380 downregulated β-catenin in the nucleus, which in turn decreased proliferation, cell cycle evolution, migration, invasion, and metastasis of NPC cells in vitro and in vivo. Concurrent accumulation of β-catenin in the cytoplasm terminated the EMT, a key mechanism in cancer cell invasiveness and metastasis, and enhanced intercellular interactions. Identification of the MNK/eIF4E/β-catenin axis provides new insight into molecular targeted treatments for NPC. These findings may help elucidate the pathway that drives NPC aggressiveness and aid development of novel MNK-eIF4E-targeting anticancer therapies.

Supplementary Material

Supplementary figures and tables.
http://www.thno.org/v07p2134s1.pdf

Acknowledgements

This work was supported by the National Natural Science Foundations of China (No: 81071820; 81272566; 81472773).

Authors' Contributions

WW designed and performed experiments and wrote the draft manuscripts. QW, JL, SC and LC helped performed the animal experiments. LX, HZ and MA analyzed data. JL and JZ assisted in the experiments. SF designed experiments and revised the paper.

Competing Interests

The authors have declared that no competing interest exists.

References

1. Le QT, Tate D, Koong A, et al. Improved local control with stereotactic radiosurgical boost in patients with nasopharyngeal carcinoma. Int J Radiat Oncol Biol Phys. 2003; 56: 1046-54.
2. Amit S, Hatzubai A, Birman Y, et al. Axin-mediated CKI phosphorylation of beta-catenin at Ser 45: a molecular switch for the Wnt pathway. Genes & Development. 2002; 16: 1066-76.
3. Rubinfeld B, Albert I, Porfiri E, et al. Binding of GSK3beta to the APC-beta-catenin complex and regulation of complex assembly. Science. 1996; 272: 1023-6.
4. Aberle H, Bauer A, Stappert J, et al. beta-catenin is a target for the ubiquitin-proteasome pathway. EMBO J. 1997; 16: 3797–804.
5. Maher MT, Mo R, Flozak AS, et al. β-Catenin Phosphorylated at Serine 45 Is Spatially Uncoupled from β-Catenin Phosphorylated in the GSK3 Domain: Implications for Signaling. Plos One. 2012; 5: e10184.
6. Cong F, Schweizer L, Varmus H. Wnt signals across the plasma membrane to activate the beta-catenin pathway by forming oligomers containing its receptors, Frizzled and LRP. Development. 2004; 131: 5103-15.
7. Gao C, Xiao G, Hu J. Regulation of Wnt/β-catenin signaling by posttranslational modifications. Cell & Bioscience. 2014; 4: 13.
8. Li VSW, Ng SS, Boersema PJ, et al. Wnt Signaling through Inhibition of β-Catenin Degradation in an Intact Axin1 Complex. Cell. 2012; 149: 1245.
9. Kumar A, Pandurangan AK, Lu F, et al. Chemopreventive sphingadienes downregulate Wnt signaling via a PP2A/Akt/GSK3β pathway in colon cancer. Carcinogenesis. 2012; 33(10): 1726-35.
10. Fang D, Hawke D, Zheng Y, et al. Phosphorylation of beta-catenin by AKT promotes beta-catenin transcriptional activity. J Biol Chem. 2007; 282: 11221-9.
11. Zhang LY, Jiang LN, Li FF, et al. Reduced beta-catenin expression is associated with good prognosis in Astrocytoma. Pathol Oncol Res. 2010; 16: 253-7.
12. Taurin S, Sandbo N, Qin Y, et al. Phosphorylation of beta-catenin by cyclic AMP-dependent protein kinase. J Biol Chem. 2006; 281: 9971-6.
13. Morin PJ, Sparks AB, Korinek V, et al. Activation of beta-catenin-Tcf signaling in colon cancer by mutations in beta-catenin or APC. Science. 1997; 275: 1787-90.
14. Leung JY, Kolligs FT, Wu R, et al. Activation of AXIN2 expression by beta-catenin-T cell factor. A feedback repressor pathway regulating Wnt signaling. J Biol Chem. 2002; 277: 21657-65.
15. Ueda T, Watanabe-Fukunaga R, Fukuyama H, et al. Mnk2 and Mnk1 are essential for constitutive and inducible phosphorylation of eukaryotic initiation factor 4E but not for cell growth or development. Mol Cell Biol. 2004; 24: 6539-49.
16. Buxade M, Parrapalau JL, Proud CG. The Mnks: MAP kinase-interacting kinases (MAP kinase signal-integrating kinases). Front Biosci. 2008; 13: 5359-73.
17. Knauf U, Tschopp C, Gram H. Negative regulation of protein translation by mitogen-activated protein kinase-interacting kinases 1 and 2. Mol Cell Biol. 2001; 21: 5500-11.
18. Wen Q, Wang W, Luo J, et al. CGP57380 enhances efficacy of RAD001 in non-small cell lung cancer through abrogating mTOR inhibition-induced phosphorylation of eIF4E and activating mitochondrial apoptotic pathway. Oncotarget. 2016.
19. Lim S, Saw TY, Zhang M, et al. Targeting of the MNK-eIF4E axis in blast crisis chronic myeloid leukemia inhibits leukemia stem cell function. Proc Natl Acad Sci U S A. 2013; 110: 2298-307.
20. Li J, Huang Y, Gao Y, et al. Antibiotic drug rifabutin is effective against lung cancer cells by targeting the eIF4E-β-catenin axis. Biochem Biophys Res Commun. 2016; 472: 299-305.
21. Jun Zheng JL, Lina Xu, Guiyuan Xie, Qiuyuan Wen, Jiadi Luo, Duo Li, Donghai Huang, Songqing Fan. Phosphorylated Mnk1 and eIF4E Are Associated with Lymph Node Metastasis and Poor Prognosis of Nasopharyngeal Carcinoma. Plos One. 2014; 9: e89220.
22. Luo W, Fang W, Li S, et al. Aberrant expression of nuclear vimentin and related epithelial–mesenchymal transition markers in nasopharyngeal carcinoma. Int J Cancer. 2012; 131: 1863-73.
23. Xiao L, Hu ZY, Dong X, et al. Targeting Epstein-Barr virus oncoprotein LMP1-mediated glycolysis sensitizes nasopharyngeal carcinoma to radiation therapy. Oncogene. 2014; 33: 4568-78.
24. Xu J, Acharya S, Sahin O, et al. 14-3-3ζ Turns TGF-β's Function from Tumor Suppressor to Metastasis Promoter in Breast Cancer by Contextual Changes of Smad Partners from p53 to Gli2. Cancer Cell. 2015; 27: 177-92.
25. Yu Y, Gaillard S, Phillip J, et al. Inhibition of Spleen Tyrosine Kinase Potentiates Paclitaxel-Induced Cytotoxicity in Ovarian Cancer Cells by Stabilizing Microtubules. Cancer Cell. 2015; 28: 82–96.

26. Wang W, Wen Q, Xu L, et al. Activation of Akt/mTOR pathway is associated with poor prognosis of nasopharyngeal carcinoma. Plos One. 2014; 9: e106098-e.
27. Li J, Guan HY, Gong LY, et al. Clinical Significance of Sphingosine Kinase-1 Expression in Human Astrocytomas Progression and Overall Patient Survival. Clin Cancer Res. 2008; 14: 6996-7003.
28. Song Y, Yang QX, Zhang F, et al. Suppression of nasopharyngeal carcinoma cell by targeting β-catenin signaling pathway. Cancer Epidemiol. 2012; 36: e116–e21.
29. Maruyama K, Ochiai A, Akimoto S, et al. Cytoplasmic beta-catenin accumulation as a predictor of hematogenous metastasis in human colorectal cancer. Oncology. 2000; 59: 302-9.
30. Fan S, Li Y, Yue P, et al. The eIF4E/eIF4G Interaction Inhibitor 4EGI-1 Augments TRAIL-Mediated Apoptosis through c-FLIP Down-regulation and DR5 Induction Independent of Inhibition of Cap-Dependent Protein Translation 1 2. Neoplasia. 2010; 12: 346-56.
31. Sun SY, Yue P, Dawson MI, et al. Differential effects of synthetic nuclear retinoid receptor-selective retinoids on the growth of human non-small cell lung carcinoma cells. Cancer Res. 1997; 57: 4931-9.
32. Cross DA. Selective small molecule inhibitors of glycogen synthase kinase-3 modulate glycogen metabolism and gene transcription. Chemistry & Biology. 2000; 7: 793.
33. Zhao Y, Zhang J, Tian Y, et al. Met tyrosine kinase inhibitor, PF-2341066, suppresses growth and invasion of nasopharyngeal carcinoma. Drug Des Devel Ther. 2014; 9: 325-32.
34. Karni R, Gus Y, Dor Y, et al. Active Src elevates the expression of beta-catenin by enhancement of cap-dependent translation. Mol Cell Biol. 2005; 25: 5031-9.
35. Wang F. Cancer cell culture—Methods and protocols. In Vitro Cell Dev-An. 2003; 39: 476-.
36. Wagh PK, Gray JK, Zinser GM, et al. β-Catenin is required for Ron receptor-induced mammary tumorigenesis. Oncogene. 2011; 30: 3694-704.
37. Polakis P. The oncogenic activation of beta-catenin. Curr Opin Genet Dev. 1999; 9: 15-21.
38. Soutto M, Peng DF, Katsha A, et al. Activation of {beta}-catenin signalling by TFF1 loss promotes cell proliferation and gastric tumorigenesis. Gut. 2015; 64: 1028-39.
39. Polakis P. Wnt signaling and cancer. Kaibogaku Zasshi. 2000; 14: 111-2.
40. Logan CY, Nusse R. The Wnt signaling pathway in development and disease. Annu Rev Cell Dev Biol. 2004; 20: 781-810.
41. Vangamudi B, Zhu S, Soutto M, et al. Regulation of β-catenin by t-DARPP in upper gastrointestinal cancer cells. Mol Cancer. 2011; 10: 1-9.
42. Yu Y, Tian L, Feng X, et al. eIF4E-phosphorylation-mediated Sox2 upregulation promotes pancreatic tumor cell repopulation after irradiation. Cancer Lett. 2016; 375: 31-8.
43. Lin W, Mei X, et al. Overexpression of nuclear β-catenin in rectal adenocarcinoma is associated with radioresistance. World J Gastroenterol. 2013; 19: 6876-82.
44. Kashino G, Liu Y, Suzuki M, et al. An alternative mechanism for radioprotection by dimethyl sulfoxide; possible facilitation of DNA double-strand break repair. J Radiat Res. 2010; 51: 733-40.
45. Jho E, Zhang T, Domon C, et al. Wnt/β-Catenin/Tcf Signaling Induces the Transcription of Axin2, a Negative Regulator of the Signaling Pathway. Mol Cell Biol. 2002; 22: 1172.
46. Chua MLK, Wee JTS, Hui EP, et al. Nasopharyngeal carcinoma. The Lancet. 2016; 387: 1012-24.
47. Chan AT, Hsu MM, Goh BC, et al. Multicenter, phase II study of cetuximab in combination with carboplatin in patients with recurrent or metastatic nasopharyngeal carcinoma. J Clin Oncol. 2005; 23: 3568-76.
48. Hui EP, Lui VWY, Wong CSC, et al. Preclinical evaluation of sunitinib as single agent or in combination with chemotherapy in nasopharyngeal carcinoma. Invest New Drugs. 2011; 29: 1123-31.
49. Hui EP, Ma BBY, King AD, et al. Hemorrhagic complications in a phase II study of sunitinib in patients of nasopharyngeal carcinoma who has previously received high-dose radiation. Ann Oncol. 2011; 22: 1280-7.
50. Truitt ML, Conn CS, Shi Z, et al. Differential Requirements for eIF4E Dose in Normal Development and Cancer. Cell. 2015; 162: 59-71.
51. Pons B, Peg V, Vazquez-Sanchez MA, et al. The effect of p-4E-BP1 and p-eIF4E on cell proliferation in a breast cancer model. Int J Oncol. 2011; 39: 1337-45.
52. Ying Y, Tao Q. Epigenetic disruption of the WNT/beta-catenin signaling pathway in human cancers. Epigenetics. 2009; 4: 307-12.
53. Fuchs SY, Ougolkov AVSpiegelman VS, Minamoto T. Oncogenic beta-catenin signaling networks in colorectal cancer. Cell Cycle. 2005; 4: 1522-39.
54. Clevers H, Nusse R. Wnt/β-Catenin Signaling and Disease. Cell. 2012; 149: 1192–205.
55. Bougnères L, Helft J, Tiwari S, et al. Nuclear localizaiton of β-catenin is associated with poor survival and chemo-/radioresistance in human cervical squamous cell cancer. Int J Clin Exp Pathol. 2014; 7: 3908-17.